High resolution pulsed infrared cavity ringdown spectroscopy: Application to laser ablated carbon clusters

Raphael Casaes, Robert Provençal,[a] Joshua Paul,[b] and Richard J. Saykally[c]
Department of Chemistry, University of California, Berkeley, California 94720

(Received 13 December 2001; accepted 25 January 2002)

We report the design and performance of a tunable, pulsed high resolution mid infrared cavity ringdown spectrometer. Stimulated Raman scattering in H_2/D_2 is used to downconvert the output of a SLM Alexandrite ring laser (720–800 nm) to the mid infrared (3–8 μm). The infrared frequency bandwidth was determined to be 90 ± 5 MHz from measurements of Doppler broadened OCS transitions at 5 μm. The minimum detectable per pass fractional absorption is 1 ppm. We observe a frequency dependent ringdown cavity transmission of ±5 ppm due to spatial variations of the mirror reflectivity. The υ_6 band of linear C_9 formed by laser ablation of graphite in a He molecular beam was measured, showing a factor of 2 improvement in sensitivity relative to previous IR diode laser experiments. Based on calculated IR intensities, the number density of C_9 in the molecular beam is $1.3*10^{11}$ molec/cm^3 and the minimum detectable density is $1*10^9$ molec/cm^3. We expect this spectrometer to be a powerful tool for the study of transient species formed in molecular beams.
 [DOI: 10.1063/1.1461825]

INTRODUCTION

Cavity ringdown spectroscopy (CRDS) has found numerous applications since its invention over a decade ago, with well over 200 recorded publications.[1] This technique has now been successfully applied to variety of systems, ranging from molecular beams and plasmas to trace gas analysis, and even solids and liquids, in the UV, VIS, and IR regions of the spectrum.[2] The development of pulsed infrared CRDS has been of particular importance for the study of transient species.[3] However, the limited resolution (1000 MHz) of currently operative and broadly tunable IR spectrometers restricts its use to the measurements of unresolved rovibrational bands for most species of interest.[4,5] Furthermore, the small absorption linewidth (20–150 MHz) of species generated in molecular beams leads to an order of magnitude decrease in detection sensitivity for such applications. To address these problems, we have designed and constructed a high-resolution pulsed infrared CRD spectrometer that is continuously tunable over most of the mid-IR (3–8 μm) with a 90 MHz bandwidth, and ca. 1 ppm fractional absorption sensitivity.

CRDS is based on the measurement of the decay rate of light trapped in a high finesse optical cavity. Since the decay rate is directly proportional to the total intracavity loss and independent of laser intensity, high sensitivity ($\sim10^{-6}$ per pass fractional absorption) direct absorption measurements are routinely achieved with pulsed lasers.[3] A number of continuous wave variants of CRDS have also been developed which significantly improve this sensitivity.[2] However, several factors influenced our decision to continue using pulsed lasers instead of cw lasers for high resolution CRDS. First and foremost is the lack of cw lasers with broad spectral coverage in the mid-infrared. Lead salt diode lasers lack continuous tunability, while color center and quantum cascade lasers have limited tunning ranges. Furthermore, cw CRDS techniques are difficult to apply to the study of a time-varying sample, such as transient species formed in molecular beams. These techniques rely on intensity buildup in the ringdown cavity, caused by constructive interference of the trapped light, followed by some method of blocking the laser so that the decay of radiation trapped in the cavity can be monitored. The intensity build up only occurs when the cavity length is a multiple of the input source's half wavelength. To ensure that this condition is met, the cavity length is typically modulated such that it sweeps over one free spectral range of the cavity,[6] leading to approximately a 100 μs timing jitter in the ringdown event relative to another event such as the initiation of a pulsed molecular beam.[7] This discourages the use of cw techniques for the study of species formed in laser ablation sources, since the sample transit time is approximately 5 μs. In the present work, the development of a pulsed high resolution infrared CRD spectrometer and its application to molecular beams are described.

LIGHT SOURCE

A pulsed Alexandrite ring laser (PAL-PRO 101, Light Age Inc.) is used to generate tunable infrared light by stimulated Raman scattering in hydrogen and deuterium (Fig. 1). The Alexandrite laser produces single longitudinal mode (SLM) pulses, 100 ns in length, and 40 MHz bandwidth. SLM operation is achieved by seeding with an external cavity diode laser (Newport) and active cavity length stabilization by an electro-optical modulator. The laser is tunable from 720 to 800 nm with pulse energies of 100 to 110 mJ

[a]Present address: Informed Diagnostics Inc, Sunnyvale, CA.
[b]Present address: Department of Chemistry, Harvard University, Cambridge MA.
[c]Author to whom correspondence should be addressed; Electronic mail: saykally@uclink4.berkeley.edu

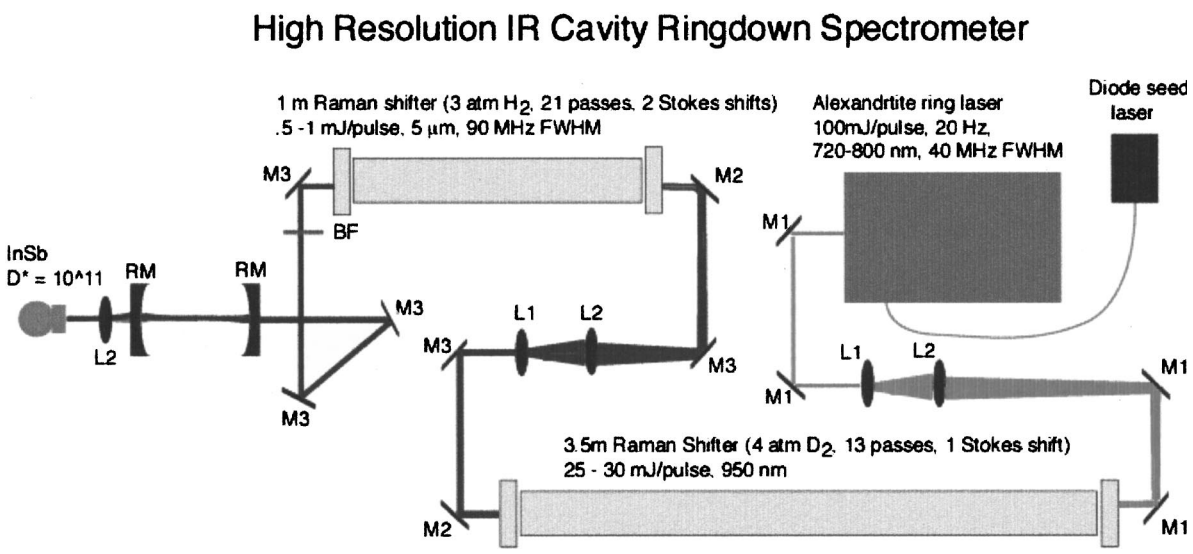

FIG. 1. High resolution pulsed infrared cavity ringdown spectrometer. Tunable pulsed infrared radiation is generated by Raman shifting an Alexandrite ring laser (100 mJ pulse energy, 40 MHz linewidth) in H_2 and D_2. Wavelength coverage is limited by the tuning range of the diode laser used to seed the Alexandrite laser, but is ultimately 1250–3751 cm^{-1}. M1=alexandrite mirror, M2=dielectric NIR mirror, M3=silver mirror, RM=ringdown mirror (R =0.9999), L1=concave lens, L2=convex lens, BF=band pass filter o.d.=7.

operating at 20 Hz. However, SLM operation is only possible if seed lasers are available. We currently operate three diode lasers covering the range from 735 to 785 nm.

Stimulated Raman scattering (SRS), first observed by Woodbury *et al.*,[8] is an efficient way to frequency shift high power pulsed lasers. Briefly, if the pump laser intensity I_L is large enough, then substantial intensity at the Stokes wavelength can develop. Under these conditions, one has to consider the simultaneous interaction of the molecules with both EM waves, the pump at frequency ω_L, and the Stokes wave with frequency $\omega_S=\omega_L-\omega_V$, where ω_V is typically the frequency of a vibrational transition in the molecule. Coupling between the two EM waves by the molecular vibration with frequency w_V leads to parametric amplification of the Stokes wave. The steady state intensity of the Stokes radiation for a pump laser intensity I_L is given by

$$I_s=I_s^0\exp(\alpha I_L z), \tag{1}$$

where α is the Raman gain factor, z is the length of the gain medium, and I_s^0 is the initial Stokes intensity.[9] The Raman gain factor α for a plane wave pump beam is proportional to the Raman scattering cross section, $d\sigma/d\Omega$, and inversely proportional to ${\omega_S}^3$. Since $d\sigma/(d\Omega)\propto\omega_L{\omega_S}^3$, $\alpha\propto\omega_L$. The exponential dependence on path-length and pump-laser intensity leads to a threshold condition for Stokes conversion, namely $I_L Z>\alpha^{-1}$. However, if no radiation is initially present at the Stokes frequency, this process amplifies the vacuum field fluctuations. As a result, in order to generate useful amounts of Stokes radiation (10^{14} photons, corresponding to 600 μJ at 5 μm), $\alpha I_L Z$ must exceed 30.[10]

The generation of multiple Stokes orders is a sequential process, wherein radiation at the Stokes frequency serves as a pump source to generate Stokes photons at frequencies $\omega_{nS}=\omega_L-n\omega_V$, $n=1,2,3,\ldots$. The Raman gain factor for each sequential Stokes shift decreases, since both the pump intensity and pump frequency decrease. This makes the generation of light shifted by $-3\omega_v$ difficult with dye and Alexandrite lasers as pump sources. Since three Stokes shifts in hydrogen or one in deuterium followed by two in hydrogen are needed to produce 3–8 μm light with these pump lasers, multipass cells are used to effectively increase the path length through the gain region.

In previous IR CRDS experiments in our group, a commercial dye laser (Lambda Physik) was used to pump a multipass hydrogen cell, generating 0.5–1 mJ third-order Stokes radiation in the mid-infrared.[11] The multipass cell increases the Raman gain by providing multiple passes through the gain medium and by refocusing the beam after each reflection. Given a Raman gain α for a collimated beam, the gain g for a focused beam is given by

$$g=\frac{4f\alpha P}{\lambda_L}\tan^{-1}\left(\frac{2l}{b}\right), \tag{2}$$

where $f=\lambda_L/(\lambda_S+\lambda_L)$, α is the plane wave gain coefficient, b is the confocal parameter of the input beam, P is the input laser power, and l is the length of the gain medium.[12] Since for a focused beam $b\ll 21$, the gain is independent of the both the pump beam confocal parameter and of the gain length. For focused beams, g is inversely proportional to $({\lambda_L}^2+\lambda_S\lambda_L)$. Although this reduces the gain relative to plane waves for long wavelength pump radiation, the advantages gained by focusing the pump beam clearly outweigh the disadvantages considering that a 2 mm diameter, 1 MW beam traveling through 1 m of H_2 at 1 atmosphere produces a Raman gain factor of 5 at 700 nm, while focusing the beam increases the gain to 55.[13] Multiple passes further increase the gain by a factor of

$$R_s^{n-1}\left(\frac{1-R_p^n}{1-R_p}\right), \tag{3}$$

TABLE I. Infrared coverage provided by stimulated Raman scattering of the Alexandrite laser. Two Raman scattering configurations are used, one Stokes shift in D_2 followed by two Stokes shift in H_2, and two Stokes shifts in D_2 followed by one Stokes shift in H_2.

λ_P	1 shift in D_2+2 shifts in H_2	2 shifts in D_2+1 shift in H_2
720–800 nm[a]	1250–2631 cm^{-1}	2363–3751 cm^{-1}
735–785 nm[b]	1437–2304 cm^{-1}	2601–3468 cm^{-1}

[a]Entire Alexandrite tuning range.
[b]Current SLM tuning range (restricted by diode seed lasers). Infrared radiation is currently tunable from 1437–3468 cm^{-1} with a gap in coverage from 2304–2601 cm^{-1}.

TABLE II. Estimated linewidth for nth Stokes radiation based on experimental parameters.

Stokes order	λ_p (nm)[a]	passes[b]	I_P (MW)[a]	G_{SRS}	$\Delta\nu_{SRS}$ (MHz)	$\Delta\nu_n$ (MHz)[c]
1	750	13	1	380	10	50
2	955	9	0.3	84	22	72
3	1560	12	0.1	76	24	96

[a]Pump wavelength and power.
[b]Number of passes.
[c]Linewidth of nth Stokes radiation for initial Alexandrite laser linewidth of 40 MHz.

where R_S and R_P are the mirror reflectivity at the Stokes and pump frequency respectively, and n is the number of passes.[14] Using a multipass cell with 98% reflectivity mirrors capable of 21 refocused passes increases the Raman gain factor for a 1 MW beam at 700 nm in 1 atmosphere of H_2 to 850.

H_2 and D_2 produce Raman shifts of 4155 and 2991 cm^{-1} respectively. Given the Alexandrite laser tuning range of 720–800 nm, a combination of stimulated Raman scattering in both H_2 and D_2 is required to generate 3–8 μm light. Therefore, the Alexandrite laser pumps a 3.5 m Herriot cell filled with 4 atm of D_2. Thirteen passes of the pump laser produces 30 mJ of first Stokes light at 917–1050 nm. This radiation is then used to pump a second 1 m Herriot cell filled with 4 atm of H_2. Twenty-one passes in this cell produces 0.5–1 mJ of second Stokes light at 1250–2631 cm^{-1}. Since SLM operation of the Alexandrite laser is currently limited to 735 to 785 nm, the actual tuning range in the infrared is restricted to 1437–2304 cm^{-1}. Conversely, by employing two Stokes shifts in D_2 followed by one Stokes shift in H_2 the infrared coverage is extended to 2601–3468 cm^{-1}. These results are summarized in Table I.

There have been several studies of the linewidth of SRS radiation and its dependence on the pump laser linewidth and the spontaneous Raman-scattering linewidth of the gain medium.[10,15,16] In the case of spontaneous Raman scattering, the linewidth of the Stokes radiation is simply the sum of the spontaneous Raman-scattering and pump-laser linewidths. However, the stimulated Raman-scattering linewidth may differ from this because of the possibility of gain narrowing. Raymer *et al.* have developed a theory of stimulated Raman scattering which treats the build up of SRS from spontaneous Raman scattering and spatial propagation through the Raman medium by using the Maxwell–Bloch equations to describe the coupling between the Stokes field operator and the molecular vibrations.[10] This treatment predicts a gain narrowed line-shape function $P_s(\omega)$ for the case where the pump laser linewidth is smaller than the spontaneous Raman scattering linewidth Γ

$$P_s(\omega)\propto\exp\left(-\frac{gI_Lz\omega^2}{\Gamma^2}\right), \tag{4}$$

where gI_LZ is the gain factor. This gives the following relationship between the stimulated ($\Delta\nu_{SRS}$) and spontaneous ($\Delta\nu_{sp}$) Raman scattered linewidths,

$$\Delta\nu_{SRS}=\Delta\nu_{sp}\sqrt{\frac{\ln 2}{\ln(G_{SRS}/2)}}, \tag{5}$$

where G_{SRS} is the total Raman gain, given by $\exp(gI_LZ)$. Subsmann *et al.* have achieved 90 MHz FWHM first Stokes radiation from 75 MHz FWHM pump pulses and H_2 pressures of 40 psi, yielding a gain narrowed SRS linewidth of 15 MHz.[15] This is in fair agreement with the 9 MHz given by Eq. (5) for $G_{SRS}=\exp(541)$, calculated from their pump beam and multipass cell parameters, and a Dicke narrowed spontaneous Raman linewidth of 250 MHz.[17]

The linewidth of each additional Stokes shift will increase, since the G_{SRS} decreases. For a given pump linewidth $\Delta\nu_L$, the linewidth of the nth Stokes beam is given by

$$\Delta\nu_{n'}=\Delta\nu_L+\sum_{n=1}^{n'}\Delta\nu_{sp}\sqrt{\frac{\ln 2}{\ln(G_{SRS}^n/2)}}, \tag{6}$$

where G_{SRS}^n is the gain for the nth order Stokes process. We can estimate the gain for the nth Stokes process in the multipass cell by measuring the energy of the $n-1$ Stokes beam after a certain number of passes i such that nth Stokes radiation is only present after $i+1$ passes. This value, and the remaining number of passes, can then be used to calculate G_{SRS}^n. Table II summarizes these parameters for $n=1-3$. This analysis predicts a linewidth of 96 MHz for the third order Stokes radiation produced in our experiment, in excellent agreement with the measured value of 90 ± 5 MHz.

COHERENCE EFFECTS

Coherence effects in the high finesse optical cavity of a CRD spectrometer have been the subject of numerous theoretical[18–20] and experimental[19–22] studies, and considerable controversy. These were motivated in part by the assertion that cavity interference effects are unimportant if the coherence length of the laser is less than the cavity length.[23] It has been shown both theoretically and experimentally that coherence effects are always present in a high finesse optical cavity, regardless of relative values of laser coherence time and cavity length.[18–22] However, in most pulsed CRDS experiments, coherence effects can be safely ignored because the laser bandwidth is significantly broader than the cavity FSR, leading to excitation of several cavity modes. The high-frequency mode beating that is present in the CRDS signal will typically be averaged out by the detector, or, in case a fast detector is used, can be electronically filtered by a 1

MHz lowpass filter. However, because several cavity modes are usually excited, the CRDS signal will be a single exponential only if the mirror reflectivity is independent of the transverse mode structure of the beam. Due to surface irregularities in the mirrors, this is usually not the case and the CRDS signal is multiexponential.

The CRDS cavity is formed by two mirrors with 6 m radius of curvature separated by 51 cm. In the case of a symmetric cavity, the cavity eigenfrequencies are given by

$$\nu_{qmn}=\frac{c}{2l}\left[q+\frac{2}{\pi}\arctan\left(\frac{l}{\sqrt{l(2r-l)}}\right)(m+n+1)\right], \quad (7)$$

where q is the longitudinal mode index, m and n are the transverse mode indices, l is the cavity length, and r is the mirror radius of curvature. The separation between longitudinal modes with the same transverse mode indices is $c/2l$, defined as the cavity free spectral range (FSR), and the separation between adjacent transverse modes, $\Delta(m+n)=1$, $\Delta q=0$, is given by $(c/\pi l)\arctan(l/(l(2r-l))\wedge.5)$. Respective cavity modes will be excited to different extents, depending on the overlap of the incident field with the cavity eigenmode structure. The total field in the cavity can be written as a linear combination of cavity eigenmodes with coefficients depending on the overlap described above:[19]

$$E(x,y,z,w)=\sum_{q}\sum_{mn} C_{mn}\Psi_{mn}(x,y,z)e_{qmn}(\omega) \quad (8)$$

$$C_{mn}=\int_{-\infty}^{\infty}\int_{-\infty}^{\infty} u(x,y,-l/2)\Psi^{*}_{mn}(x,y,-l/2)\partial x\partial y \quad (9)$$

$$e_{qmn}(\omega)=\mathrm{H}_{qmn}(\omega)e(\omega). \quad (10)$$

Here C_{mn} is the spatial coupling coefficient between the incident field $u(x,y,z)$ spatial structure and the cavity transverse modes Ψ_{mn}, while $e_{qmn}(\omega)$ is the frequency coupling coefficient involving the cavity response function $H_{qmn}(\omega)$ and the incident field spectral structure $e(\omega)$.[19]

In the case of a broadband laser pulse, wherein the field bandwidth overlaps several TEM_{mn} cavity modes, the spatial structure of the cavity field will be essentially independent of the incident field center frequency. To illustrate this, assume a cavity formed by mirrors with unit reflectivity and no losses due to absorption or diffraction. In this case, the cavity response function, $\mathrm{H}_{qmn}(\omega)$, will be a comb of delta functions at frequencies given by Eq. (7). If we restrict the analysis to a single transverse mode, then the total cavity response for that particular transverse mode is[19]

$$H_{mn}(\omega)=\sum_{q} H_{qmn}(\omega). \quad (11)$$

Here the response function is a comb of delta functions separated by the cavity FSR. If we apply this function to a field whose power spectrum is three times the cavity FSR, typical for dye lasers with 900 MHz bandwidth and 50 cm ringdown cavities, centered at a cavity eigenfrequency ω' of a TEM_{mn} mode, we find that $e_{mn}(\omega')/e_{mn}(\omega'+\mathrm{FSR}/2)=0.9996$. Clearly, for this case $e_{mn}(\omega)$ is essentially constant and the transverse mode structure of the field in the cavity will depend only on the spatial coupling coefficients C_{mn}. This situation is illustrated in Fig. 2.

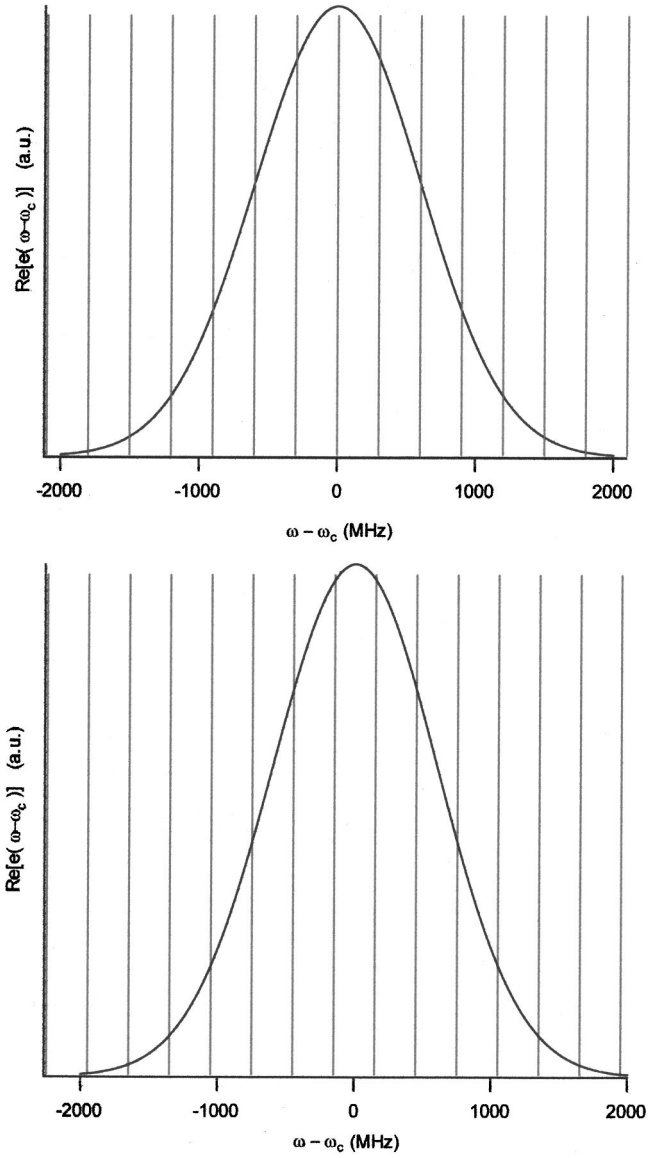

FIG. 2. Overlap of a broadband laser pulse with the cavity response function for a single TEM_{mn} mode. For simplicity, cavity response function is assumed to be a comb of delta functions. Top: Input field centered at a cavity eigenfrequency of a TEM_{mn} mode. Bottom: Input field centered in-between two cavity eigenfrequencies. Overlap is essentially independent of the input field center frequency.

Figure 3 illustrates the case for a pulse with 100 MHz bandwidth. Here it is clear that $e_{mn}(\omega)$ is not constant. When ω' is an eigenfrequency of a cavity TEM_{mn} mode, $e_{mn}(\omega)$ will be a maximum, indicating strong coupling to that TEM_{mn} mode, while at a frequency $\omega'-\mathrm{FSR}/2$, $e_{mn}(\omega)$ will be zero. As a result, the transverse mode structure of the field in the cavity will be a function of the incident field center frequency. If the incident field is mode matched to the cavity TEM_{00} mode, or if the cavity is constructed in such a way as to maximize diffraction losses for higher-order transverse modes, the cavity will act as an etalon, transmitting light only at frequencies ω' that are eigenfrequencies of the cavity

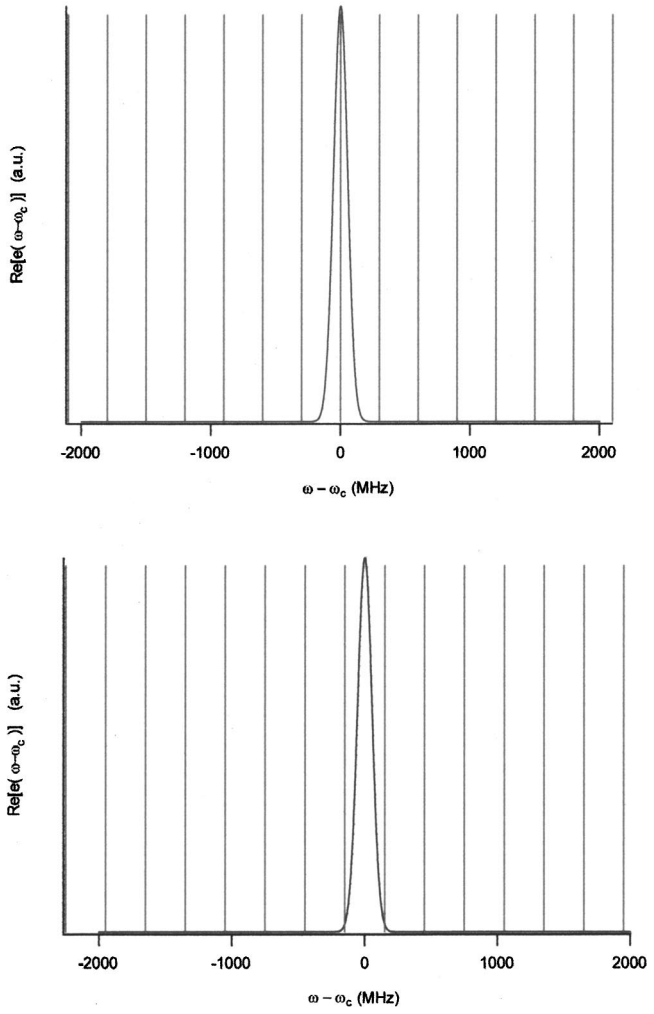

FIG. 3. Overlap of a narrowband laser pulse with the cavity response function for a single TEM_{mn} mode. For simplicity cavity response function is assumed to be a comb of delta functions. Top: Input field centered at a cavity eigenfrequency of a TEM_{mn} mode showing maximum overlap. Bottom: Input field centered in between two cavity eigenfrequencies, showing zero overlap.

TEM_{00} modes. Hodges *et al.* have observed this effect by placing an intracavity aperture to increase the diffraction losses of higher order TEM_{mn} modes.[19]

In order to perform high resolution pulsed cavity ringdown experiments, one may either mode match the incident beam to the cavity TEM_{00} mode and scan the cavity length as the laser wavelength is scanned, or intentionally not mode match the incident beam to ensure that the spatial coupling coefficients for $m+n>0$ are nonzero. The former ensures single mode excitation and single-exponential decay, with the significant complication of cavity length stabilization and scanning, while the later requires no cavity stabilization at the expense of single mode excitation. We have chosen not to mode match the beam to the cavity because of the difficulty involved in locking the cavity to a pulsed laser. Figure 4 shows per pass fractional losses versus frequency taken with an empty cavity. Several groups have observed the baseline oscillations, which are spaced by the cavity FSR.[24–26] These are due to a dependence of the mirror reflectivity on the transverse mode structure of the beam, caused by inhomogeneities in the mirror surface. Since $e_{qmn}(\omega)C_{mn}$ is an oscillating function of ω with a period equal to the cavity FSR, the decay rate measured in the ringdown experiment will also be an oscillating function of ω with period equal to the cavity FSR. These oscillations can easily be removed in the data analysis by fitting them to an oscillating function and subtracting, or by recording the spectrum of the empty cavity and subtracting it from the spectrum containing the species of interest.

SENSITIVITY

The sensitivity of CRDS depends on the mirror reflectivity R and on the accuracy in the determination of the ringdown time τ, defined as the time it takes for the intensity to decay to $1/e$ of its initial value. The minimum detectable fractional absorption can be expressed in terms of these two parameters as

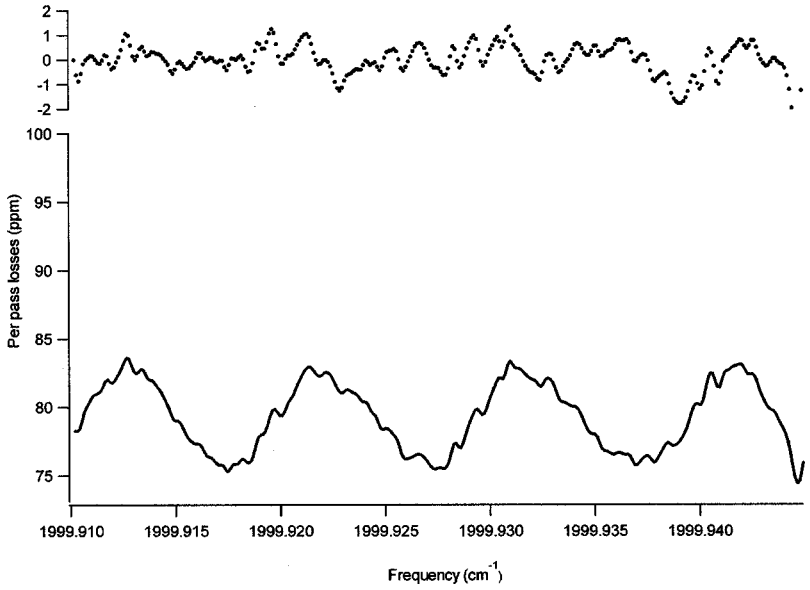

FIG. 4. Baseline oscillations. The baseline oscillations are most likely due to a reflectivity dependence on the transverse mode structure of the beam. The crests in the oscillation are separated by the cavity's FSR (approximately 300 MHz). On top the residuals of a fit to a sine function are plotted.

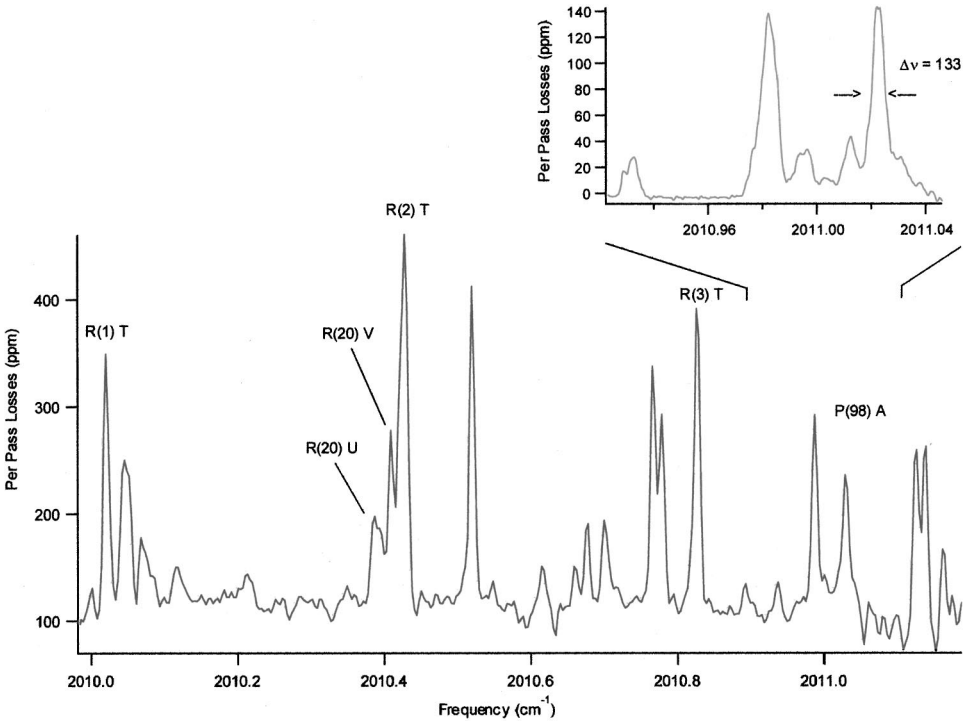

FIG. 5. Spectra of the OCS ν_1 vibrational band taken with the high-resolution infrared cavity ringdown spectrometer. The large spectrum was taken in fast scanning mode (100 MHz step size). Inset shows a background subtracted region scanned with 10 MHz step size demonstrating an experimental resolution of 133 MHz, corresponding to a laser bandwidth of 90 MHz. A. $^{16}O\,^{12}C\,^{32}S\ 10^00-00^00$; T. $^{16}O\,^{13}C\,^{32}S\ 10^00-00^00$; U. $^{16}O\,^{13}C\,^{32}S\ 11^10-01^{1e}0$; V. $^{16}O\,^{13}C\,^{32}S\ 11^10-01^{1f}0$.

$$A_{\min}=(1-R)\left(\frac{\Delta\tau}{\tau}\right)_{\min}. \tag{12}$$

Equation (12) shows why CRDS is a highly sensitive technique: In order to effect high sensitivity in the absorption measurement, a relatively low accuracy in the time measurement is needed. For example, with 99.99% reflectivity mirrors, an accuracy of 1% in the determination of τ is needed to achieve a minimum detectable fractional absorption of 10^{-6} per pass.

Noise sources in CRDS, which lead to errors in the determination of τ, can be divided into three categories, multimode cavity excitation leading to multiexponential decays, technical noise, arising from electrical noise in the detector and amplifier and from finite vertical resolution of the digitizer, and shot noise.[27] Most pulsed ringdown experiments report ca. 1% accuracy in the determination of τ, which is primarily due to multimode excitation of the ringdown cavity. Recently, van Zee *et al.*[27] reported an accuracy of 0.03% in the determination of τ by exciting a single cavity mode using a seeded OPO and a temperature regulated ringdown cavity with longitudinal and transverse mode spacing of 1500 and 500 MHz, respectively. It was determined that the dominant noise source in their experiment was technical noise and, if the shot noise limit were actually achieved, the accuracy in the determination of τ would be 0.003%.

Two hurdles must be overcome in order to achieve single mode excitation in CRDS. First, the cavity length must be stabilized. Since $dl/l=d\omega/\omega$, the cavity length variations must be <75 nm in order to achieve a 10 MHz frequency stability in the mid-infrared. Second, the cavity length must track the laser frequency as it is swept, such that the input source power spectrum always overlaps a cavity TEM_{00} mode. The first hurdle is difficult to overcome in experiments employing pulsed molecular beams, since in these experiments, the large density gradient present in the cavity will induce a phase shift in the propagating field. This phase shift will vary from pulse to pulse due to instabilities in the molecular beam (this is especially true in laser ablation sources, wherein a dense plasma is formed). Thus, the cavity length would have to be actively locked to the input laser in order to account for the varying phase shift. Of course, the second hurdle would also be overcome by actively locking the cavity length. Unfortunately, there are no cw light sources in our experiment that would allow us to actively lock the cavity to the laser. Thus, we have decided to operate in the multiexponential regime, leading to a routinely achievable minimum detectable fractional absorption of $\sim 10^{-6}$ per pass once the baseline oscillations are subtracted out. Nevertheless, this is an impressive sensitivity for a direct absorption experiment, especially considering that such measurements can be made in ca. 20 μs.

APPLICATIONS

The tunable, pulsed IR output from the Raman shifter was used to perform IR-CRDS experiments in both a flow cell and in a supersonic molecular beam plasma. Approximately 1 mJ of 5 μm light pulses with a a repetition rate of 20 Hz were injected into a ringdown cavity formed by two highly reflective mirrors ($R=99.99\%$ at 5 μm, Laser Power Optics) with 6 m radius of curvature separated by 51 cm. A band pass filter, o.d.$=7$ (OCLI), was used to block the ancillary frequency produced in the SRS process (first and second Stokes, anti-Stokes, and frequencies due to rovibrational transitions in H_2). The light exiting the cavity was focused onto the 2 mm element of a 1 MHz LN cooled InSb detector ($D^*=10^{11}$, Infrared Associates), amplified, digitized, and

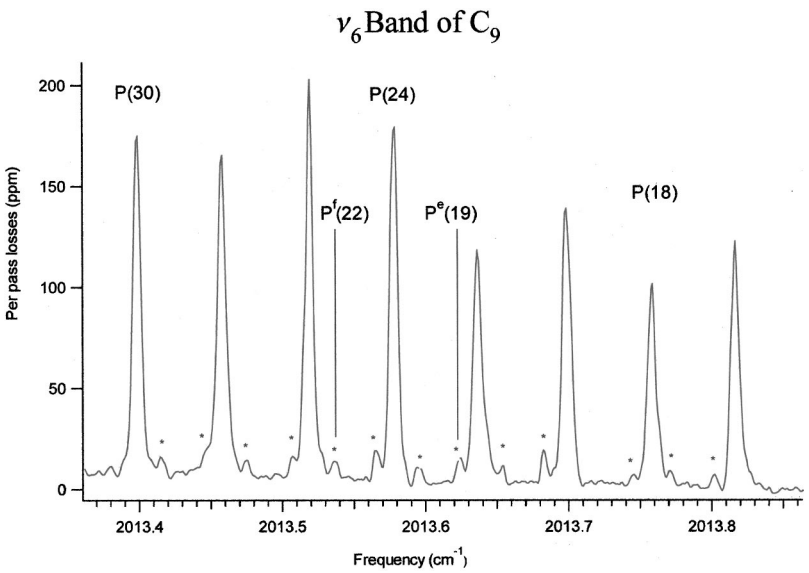

FIG. 6. ν_6 band of linear C_9. Carbon clusters are formed by 355 nm laser ablation of a graphite target seeded in a helium supersonic expansion. Peaks labeled with an asterisk are due to hot band transitions arising from vibrationally excited bending modes. A Doppler broadened linewidth of 180 MHz is measured for these transitions.

sent to a PC for analysis. Ringdown times were calculated from a fit of the ringdown decay to a single exponential.

Rovibrational spectra of the OCS υ_1 band and υ_1 ($\upsilon_2 = 1$) hot band of $^{16}O\,^{13}C\,^{32}S$ isotopomer were taken by flowing a mixture of 3% OCS in helium through the ringdown cavity. The pressure in the cavity was maintained at 30 mTorr by adjusting the flow rate with a needle valve. Figure 5 shows CRD spectra of the several transitions of OCS lying near 2010 cm^{-1}. The large spectrum is a fast scan with step size of 100 MHz. The inset shows a background subtracted region scanned with a 10 MHz step size, demonstrating an experimental linewidth of 133 MHz. Deconvolution employing a 98 MHz FWHM room temperature Doppler broadened lineshape yields a laser bandwidth of 90 MHz. The baseline noise is ± 0.5 ppm, resulting in a minimum detectable per pass fractional absorption of 1 ppm.

Figure 6 shows CRD spectrum of the ν_6 band of the linear C_9 cluster. The carbon cluster source employed here has been described in detail previously.[28] Briefly, carbon clusters are produced by laser ablation of graphite followed by supersonic expansion in a He molecular beam, using 100 mJ at 355 nm from a Nd:Yag laser (Continum) focused to a line on the graphite rod. The rod is translated and rotated to ensure that the ablation is uniform. Helium at 200 psi backing pressure flows over the graphite rod and into a flared channel (0.8 cm long and 1 cm wide at the end) before entering the vacuum chamber. A solenoid valve (General Valve) is used to pulse the molecular beam at 20 Hz and the chamber pressure is kept at 60 mTorr by a Roots blower pump. This source produces rotationally cold (~20–40 K) carbon clusters with vibrational temperatures that depend on the ablation laser fluence.

The cluster beam has a 5 μs pulse width and crosses the optical axis 15 μs after the ablation laser is fired. The short transit time reduces the sensitivity of the CRDS experiment by ca. 2 ppm, but allows for active background subtraction.

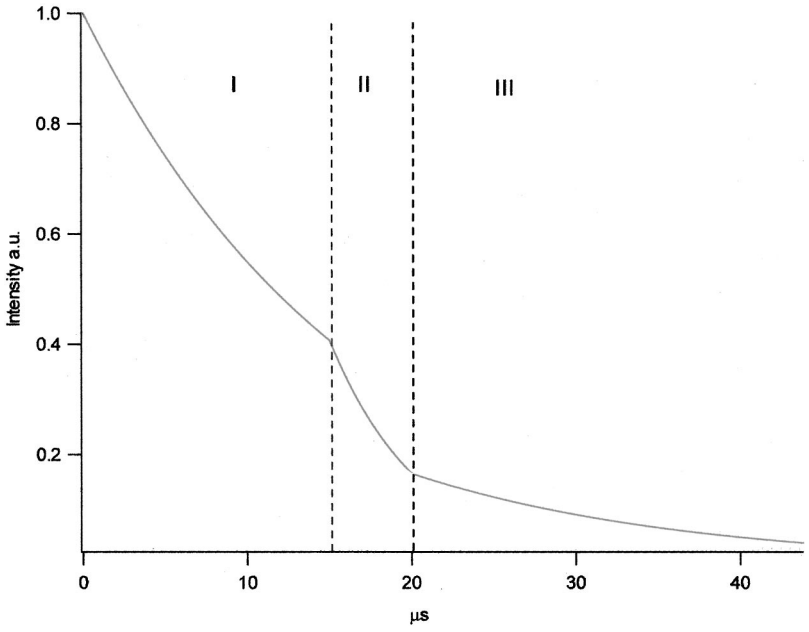

FIG. 7. Detector output for a carbon cluster absorption. The intensity decay can be divided into three regions: I. Before clusters cross the optical axis. II. Clusters present on the optical axis. III. After clusters cross the optical axis. Cavity losses due to carbon cluster absorption are measured by subtracting the averaged cavity losses in regions I and III from the cavity losses in region II. This effectively removes the baseline oscillations shown in Fig. 4.

Since the cluster beam is only present for 5 μs, the cluster absorption signal is derived from an exponential fit to a 5 μs time window of the detector output. Fits to two other time windows, one before and one another after the clusters cross the optical axis, are used to compute the background losses, which are then averaged and subtracted from the cluster signal (Fig. 7).

Because ^{12}C atoms are bosons, the C_9 wave function must be symmetric with respect to exchange of nuclear coordinates. Since the electronic, vibrational, and nuclear spin ground state wave functions are symmetric, only even values of J are allowed in the ground state. Peaks labeled with an asterisk are due to hot band transitions arising from vibrationally excited bending states (one quanta excited in the ν_{15} mode). As the ν_{15} mode is a degenerate mode, it gives rise to vibrational angular momentum, and the interaction between vibrational and rotational angular momenta splits the degenerate bending states into symmetric and antisymmetric components. For the symmetric component, denoted by a superscript *f*, only even values of J are allowed, while for the antisymmetric component, denoted by a superscript *e*, only odd values of J are allowed. Although relative intensities are not accurate enough to calculate the rotational temperature by using the relation $\ln[I(J)/(J+1)]=-(B/kT)^*J(J+1)$, the rotational temperature can be estimated from the region of maximum absorption in the spectrum by using the expression $T=(2B/k)^*(J_{\max}+0.5)\,2$. Since this occurs at P(26), and using published values for the rotational constant in the ground vibrational state of .0143 cm^{-1}, we estimate a rotational temperature of 29 ± 5 K. From this temperature, the P(26) integrated line intensity, a 1 cm path length (the source exit slit width), and a calculated band intensity of 2628 km/mole,[29] we calculate a C_9 average density in the molecular beam of 1.3×10^{11} molecules/cm^3. The signal to noise ratio is twice that obtained from previous infrared diode laser experiments under similar source conditions,[30] with the added advantage of continuous frequency coverage and improved frequency stability. The minimum detectable number density of C_9 in the molecular beam is 1×10^9 molecules/cm^3, making this spectrometer a powerful tool for high-resolution studies of laser ablated species.

CONCLUSIONS

We have described the design and performance of a high-resolution pulsed infrared cavity ringdown spectrometer that is tunable over most of the mid-infrared. The IR frequency bandwidth has been determined to be 90 MHz from measurements of Doppler broadened OCS transitions at 5 μm. The ringdown cavity was not length stabilized and no efforts were made to mode match the input laser to the cavity TEM_{00} mode. As a result the cavity transmission was independent of the laser center frequency, i.e., it behaved as a ''white'' cavity, except for small oscillations due to mirror reflectivity dependence on the field transverse mode structure. The ν_6 band of linear C_9, formed by laser vaporization of graphite followed by supersonic expansion, was shown to exhibit a factor of two improvement in sensitivity relative to previous IR diode laser absorption experiments. We expect this spectrometer design to be quite powerful for a number of spectroscopic investigations.

ACKNOWLEDGMENTS

The Berkeley Pulsed High Resolution CRDS effort was initially funded by the Chemical Dynamics Program of the AFOSR, and is currently supported by the experimental Physical Chemistry Division of the NSF and the Astrophysics and Exobiology Programs of NASA. The authors thank Dr. John Walling and the management of Light Age Inc. for their invaluable help in perfecting the Alexandrite laser system for this application.

[1] A. O'Keefe and D. A. G. Deacon, Rev. Sci. Instrum. **59**, 2544 (1988).
[2] G. Berden, R. Peeters, and G. Meijer, Int. Rev. Phys. Chem. **19**, 565 (2000).
[3] J. J. Scherer, J. B. Paul, A. O'Keefe, and R. J. Saykally, Chem. Rev. **97**, 25 (1997).
[4] R. A. Provencal, R. N. Casaes, K. Roth, J. B. Paul, C. N. Chapo, R. J. Saykally, G. S. Tschumper, and H. F. Schaefer, J. Phys. Chem. A **104**, 1423 (2000).
[5] J. B. Paul, R. A. Provencal, C. Chapo, A. Pettersson, and R. J. Saykally, J. Chem. Phys. **109**, 10201 (1998).
[6] B. A. Paldus, C. C. Harb, T. G. Spence *et al.*, Opt. Lett. **25**, 666 (2000).
[7] M. Hippler and M. Quack, Chem. Phys. Lett. **314**, 273 (1999).
[8] E. J. Woodbury and W. K. Ny, IRE Proc **50**, 2367 (1962).
[9] M. Maier, Appl. Phys. **11**, 209 (1976).
[10] M. G. Raymer and J. Mostowski, Phys. Rev. A **24**, 1980 (1981).
[11] J. B. Paul, C. P. Collier, R. J. Saykally, J. J. Scherer, and A. O'Keefe, J. Phys. Chem. A **101**, 5211 (1997).
[12] P. Rabinowitz, A. Stein, R. Brickman, and A. Kaldor, Opt. Lett. **3**, 147 (1978).
[13] J. Paul (unpublished).
[14] P. Rabinowitz, B. N. Perry, and N. Levinos, IEEE J. Quantum Electron. **QE-22**, 797 (1986).
[15] R. Sußmann, T. Weber, E. Riedle, and H. J. Neusser, Opt. Commun. **88**, 408 (1992).
[16] D. V. Guerra and R. B. Kay, J. Phys. B **26**, 3975 (1993).
[17] A. Owyoung, Opt. Lett. **2**, 91 (1978).
[18] K. K. Lehmann and D. Romanini, J. Chem. Phys. **105**, 10263 (1996).
[19] J. T. Hodges, J. P. Looney, and R. D. van Zee, J. Chem. Phys. **105**, 10278 (1996).
[20] P. Zalicki and R. N. Zare, J. Chem. Phys. **102**, 2708 (1995).
[21] J. T. Hodges, J. P. Looney, and R. D. van Zee, Appl. Opt. **35**, 4112 (1996).
[22] J. Martin, B. A. Paldus, P. Zalicki, E. H. Wahl, T. G. Owano, J. S. Harris, C. H. Kruger, and R. N. Zare, Chem. Phys. Lett. **258**, 63 (1996).
[23] J. J. Scherer, D. Voelkel, D. J. Rakestraw, J. B. Paul, C. P. Collier, R. J. Saykally, and A. O'Keefe, Chem. Phys. Lett. **245**, 273 (1995).
[24] M. G. H. Boogaarts and G. Meijer, J. Chem. Phys. **103**, 5269 (1995).
[25] H. Naus, A. deLange, and W. Ubachs, Phys. Rev. A **56**, 4755 (1997).
[26] D. Romanini and K. K. Lehmann, J. Chem. Phys. **102**, 633 (1995).
[27] R. D. van Zee, J. T. Hodges, and J. P. Looney, Appl. Opt. **38**, 3951 (1999).
[28] A. Van Orden and R. J. Saykally, Chem. Rev. **98**, 2313 (1998).
[29] J. M. L. Martin, J. P. Francois, and R. Gijbels, J. Chem. Phys. **93**, 8850 (1990).
[30] A. Van Orden, Ph.D. thesis, University of California, 1996.